Available online at www.sciencedirect.com
ScienceDirect
Journal of Sound and Vibration 303 (2007) 526–537
JOURNAL OF SOUND AND VIBRATION
www.elsevier.com/locate/jsvi

Exact dynamic stiffness method for non-uniform Timoshenko beam vibrations and Bernoulli–Euler column buckling

Si Yuan[a], Kangsheng Ye[a], Cheng Xiao[a], F.W. Williams[b], D. Kennedy[b,*]

[a]*Department of Civil Engineering, Tsinghua University, Beijing 100084, China*
[b]*Cardiff School of Engineering, Cardiff University, Cardiff CF24 3AA, UK*

Received 14 September 2005; received in revised form 12 October 2006; accepted 15 January 2007

Abstract

The exact dynamic stiffness method is further extended, using a recently developed approach for vibration of Bernoulli–Euler members, to flexural free vibration of non-uniform Timoshenko beams with gradual or stepwise non-uniformity of geometric and/or material properties and to Euler buckling of similarly non-uniform columns. Two key strategies are emphasized: (i) formulation of the governing ordinary differential equations (ODE) for dynamic stiffnesses and their derivatives and the solution of the ODE problem by standard ODE solvers; and (ii) establishment of mesh generation rules for the two problems. Extension of the method to three-dimensional frames with non-uniform members poses no major theoretical hurdles. Numerical examples, including challenging problems, are given to show the effectiveness, efficiency, accuracy and reliability of the proposed method which, unlike the finite element method, is exact and so can be iterated until any preset accuracy is achieved.

1. Introduction

1.1. Theory used

When using exact methods for undamped free vibration of structures, the generalized linear eigenproblem $(\mathbf{K}-\lambda\mathbf{M})\mathbf{D}=\mathbf{0}$ of approximate methods such as the finite element method (FEM) is replaced by the transcendental eigenproblem [1,2]

$$\mathbf{K}(\lambda)\mathbf{D}=\mathbf{0}. \tag{1}$$

Here, $\lambda=\omega^2$; ω is the circular frequency; $\mathbf{D}$ is the displacement amplitude vector (simply called the mode vector in the following) and so must be multiplied by $\sin(\omega t)$ to obtain the displacements; $\mathbf{M}$ and $\mathbf{K}$ are the mass and static stiffness matrices; and $\mathbf{K}(\lambda)$ is the dynamic stiffness matrix. The coefficients of $\mathbf{K}(\lambda)$ are transcendental functions involving λ and mass because the members of the structure are analysed exactly by solving their governing differential equations. Note that this formulation, and the Wittrick–Williams (W–W)

*Corresponding author. Tel.: +44 29 2087 5340; fax: +44 29 2087 4939.
E-mail address: kennedyd@cf.ac.uk (D. Kennedy).

0022-460X/$ - see front matter © 2007 Elsevier Ltd. All rights reserved.
doi:10.1016/j.jsv.2007.01.036

algorithm referred to next, cover the full range of members for which transcendental member equations are available but that in this paper the word 'member' is used more restrictively to mean a beam in vibration problems or a column in buckling ones.

It was shown in a recent paper [3] that the natural frequencies and modes can be found with absolute certainty and to almost machine accuracy by a method which uses the W–W algorithm [1,2] in conjunction with a form of inverse iteration. This method, after slight modification to use λ rather than ω as the eigenparameter [4], requires as its raw material $\mathbf{K}(\lambda)$ and its first derivative with respect to λ, namely $\hat{\mathbf{K}}(\lambda) = \mathrm{d}\hat{\mathbf{K}}(\lambda)/\mathrm{d}\lambda$, plus a quantity J which is equal to the number of natural frequencies exceeded by any trial value of λ, denoted by λ^*. (Note that prime is not used to denote the derivative here because later it is used to denote differentiation with respect to x.) J is computed from a property of $\mathbf{K}(\lambda^*)$ and from J_m for every member, where J_m is the number of natural frequencies of the member which would lie below λ^* if its ends were both fully clamped. $\mathbf{K}(\lambda)$ and $\hat{\mathbf{K}}(\lambda)$ are respectively assembled from the member flexural stiffnesses k_{ij} ($i, j = 1, 2, 3, 4$) of all component members of the structure, plus their axial stiffnesses, and from their derivatives $\hat{k}_{ij}$ with respect to λ. This use of k_{ij} and $\hat{k}_{ij}$, plus the computation of J_m, forms the only member information required by the recent inverse iteration method [3,4] and hence the method can be applied when using any type of member for which $k_{ij}, \hat{k}_{ij}$ and J_m can be computed and for which the axial and flexural behaviours are uncoupled.

1.2. Introduction to method presented

The method includes a check that no fixed-end eigenvalue of any member lies very close to λ^*, as otherwise the $\hat{k}_{ij}$ could become excessively numerically large and hence potentially make the inverse iteration method unstable. When this check is violated, an interior node is inserted into the member and is located such that the two sub-members thus formed both pass this check. Such interior nodes must also be placed wherever there is a stepped non-uniformity of the member.

The first and primary objective of the present paper is to introduce a numerical ordinary differential equation (ODE) solver in order to find the k_{ij} and $\hat{k}_{ij}$ of isolated vibrating Timoshenko beams with gradual or stepwise non-uniformity of geometric and/or material properties. For such members it is no longer easy to calculate J_m from an explicit formula. Therefore the previously applied 'necessary and sufficient' condition for ensuring that the $\hat{k}_{ij}$ do not become excessive, namely ensuring that no fixed-end eigenvalue lies very close to λ^*, is replaced by a strategy which ensures that the square of the lowest fixed-end natural frequency of the non-uniform member, denoted by λ_F, lies above λ^*, so that $J_m = 0$ and hence the quantity J_0 [3] needed by the W–W algorithm is zero. This is achieved by developing a method which makes sure that sufficient interior nodes are introduced to ensure that the sub-members into which they divide the member all have $\lambda_F > \lambda^*$. In this paper, the sub-members are called elements and the interior nodes are called mesh points. Hence one of the most important contributions of the present paper is that it introduces a criterion for ensuring that $\lambda_F > \lambda^*$ for all of the Timoshenko elements, after first showing how to compute their k_{ij} and $\hat{k}_{ij}$. It also solves some examples which confirm the efficiency and the very high accuracy of the method, which is essentially exact if an adaptive ODE solver is used properly. (Exceptionally, a non-uniform member may contain long uniform portions, so that one or more elements may be uniform. Extra care is then needed as very exceptionally the condition $\lambda_F > \lambda^*$ may result in $\lambda_F \cong \lambda^*$ and so cause ill-conditioning. This difficulty is easily overcome in several ways, one of which is to modify the condition to $\lambda_F > (1+\varepsilon)\lambda^*$, where ε is a suitable small number, e.g. 0.01 or 0.05.)

The second objective of the paper is to present a method for buckling of non-uniform columns which follows the same route as that described above for vibration of such members. This is possible because the close analogy between vibration and buckling enables the previously presented method [3,4] for vibration problems to be readily adapted to solve critical buckling problems. Moreover, essentially everything said thus far in this paper applies also to buckling problems if λ is interpreted as the axial force, the squares of natural frequencies become critical buckling loads, $\mathbf{M}$ becomes the geometric stiffness matrix and 'dynamic stiffnesses' are replaced by their equivalents for buckling problems, which are widely known as 'stability functions'. However, for practical rather than fundamental reasons, and because it is only secondary in this paper, the detailed working for buckling has only been done for Bernoulli–Euler columns and not for Timoshenko ones,

i.e. shear deflection is ignored. Thus the presented method includes a method for finding the k_{ij} and $\hat{k}_{ij}$, plus a guarantee that elements all have $\lambda_F > \lambda^*$, for flexure of a static non-uniform Bernoulli–Euler beam with a compressive force P, which may be positive, zero or negative.

Note that axial vibration of non-uniform beams involves a second-order Sturm-Liouville (SL) problem for which several general codes are available, e.g. SLEDGE [5], SLEIGN [6] and the NAG library [7]. Similarly the more challenging fourth-order SL problem can be solved by SLEUTH [8] and this is sufficient for vibrating non-uniform Bernoulli–Euler beams. However, the governing differential equations for flexure of the two types of member described in this paper are not SL ones, which is one of the reasons for choosing them in this paper. In this paper, the linear ODE boundary value problems (BVP) yielded by fixing $\lambda = \lambda^*$ are instead solved by any available and reliable standard ODE solver, with COLSYS [9] being used exclusively in this paper. Hence the stiffness derivatives $\hat{k}_{ij}(= \hat{k}_{ij}(\lambda^*))$ are calculated by differentiating the governing ODE for k_{ij} with respect to λ at $\lambda = \lambda^*$ to obtain a new linear ODE problem, which can be solved to obtain the $\hat{k}_{ij}$ in the same easy way as that used to calculate the k_{ij}.

Note both that COLSYS uses spline collocation at Gaussian points to directly solve ODE systems of first to fourth order and also that its meshes are automatically generated and adapted according to error distributions until the user pre-specified error tolerance is satisfied. Although this is not a closed form solution it is numerically exact so long as the flexural rigidity and mass per unit length vary smoothly along members.

The theory currently presented and the associated software are specifically for the chain of collinear non-uniform elements required to assemble a single non-uniform member, which requires the following derivations of the exact member flexural stiffness matrices of the vibrating Timoshenko beam and the static Bernoulli–Euler column. However, it must be emphasised that the ultimate motivation is the calculation of the natural frequencies or critical buckling loads of three-dimensional frameworks of any geometry which contain non-uniform members, with an emphasis on the associated modes being found to high accuracy. The hardest step in the theory for such frameworks is the derivation of the exact member flexural stiffness matrices given in the next two sections. The remaining theory needed for the solution of three-dimensional frameworks comprising members with uncoupled flexural, axial and torsional behaviour is much simpler, e.g. it is necessary: to derive exact member axial stiffness matrices; to superpose flexure in two principal planes with the axial and torsional equations to obtain the required member equations; and to perform a standard transformation to resolve member end displacements and forces into a global axis system, exactly as in the application of the stiffness matrix method to standard finite element problems.

2. Exact flexural stiffness matrix and its derivative for vibrating non-uniform Timoshenko beams

The stiffnesses k_{ij} $(i, j = 1, 2, 3, 4)$ for flexural vibration of a non-uniform Timoshenko member (or element) are calculated by solving the following second-order linear ODE BVP of Eq. (2) subject to the four sets of boundary conditions (BCs) of Eq. (3):

$$\left.\begin{aligned} &\frac{\mathrm{d}}{\mathrm{d}x}\left(\mathrm{EI}(x)\frac{\mathrm{d}\psi}{\mathrm{d}x}\right) + \kappa\mathrm{GA}(x)\left(\frac{\mathrm{d}v}{\mathrm{d}x} - \psi\right) + \lambda^* I_m(x)\psi = 0 \\ &\frac{\mathrm{d}}{\mathrm{d}x}\left[\kappa\mathrm{GA}(x)\left(\frac{\mathrm{d}v}{\mathrm{d}x} - \psi\right)\right] + \lambda^* m(x)v = 0 \end{aligned}\right\}, \quad 0 < x < L, \tag{2}$$

$$j = 1: \quad v_j(0) = 1, \quad \psi_j(0) = 0, \quad v_j(L) = 0, \quad \psi_j(L) = 0, \tag{3a}$$

$$j = 2: \quad v_j(0) = 0, \quad \psi_j(0) = 1, \quad v_j(L) = 0, \quad \psi_j(L) = 0, \tag{3b}$$

$$j = 3: \quad v_j(0) = 0, \quad \psi_j(0) = 0, \quad v_j(L) = 1, \quad \psi_j(L) = 0, \tag{3c}$$

$$j = 4: \quad v_j(0) = 0, \quad \psi_j(0) = 0, \quad v_j(L) = 0, \quad \psi_j(L) = 1. \tag{3d}$$

Here (x) denotes variation with the longitudinal coordinate x; L is the member length; $v(x)$ and $\psi(x)$ (or just v and ψ) are the amplitudes of, respectively, the lateral deflection and cross-section rotation; $\mathrm{EI}(x)$ and $\mathrm{GA}(x)$ are, respectively, the flexural and shear rigidities; $m(x)$ and $I_m(x)$ are, respectively, the mass and rotary inertia

per unit length; and κ is the standard cross-section constant, which is given its usual value for rectangular cross-sections of 5/6 in the numerical examples of this paper. Note that the ODE problem consists of a set of two differential equations rather than the single equation needed for vibration of Bernoulli–Euler members.

After the solutions have been obtained for $j = 1$, 2, 3, and 4, the dynamic stiffnesses can readily be calculated from

$$\left.\begin{aligned} k_{1j} &= -\kappa GA\left(\frac{dv_j}{dx} - \psi_j\right)\Big|_0, \quad k_{2j} = -EI\frac{d\psi_j}{dx}\Big|_0 \\ k_{3j} &= \kappa GA\left(\frac{dv_j}{dx} - \psi_j\right)\Big|_L, \quad k_{4j} = EI\frac{d\psi_j}{dx}\Big|_L \end{aligned}\right\}, \quad j = 1,2,3,4. \tag{4}$$

The $\hat{k}_{ij}(i,j = 1,2,3,4)$ are then obtained by letting $\hat{v} = \partial v/\partial\lambda$ and $\hat{\psi} = \partial\psi/\partial\lambda$, so that differentiating Eqs. (2) and (3) with respect to λ gives

$$\left.\begin{aligned} &\frac{d}{dx}\left(EI(x)\frac{d\hat{\psi}_j}{dx}\right) + \kappa GA(x)\left(\frac{d\hat{v}_j}{dx} - \hat{\psi}_j\right) + \lambda^* I_m(x)\hat{\psi}_j = -I_m(x)\psi_j \\ &\frac{d}{dx}\left[\kappa GA(x)\left(\frac{d\hat{v}_j}{dx} - \hat{\psi}_j\right)\right] + \lambda^* m(x)\hat{v}_j = -m(x)v_j \end{aligned}\right\}, \quad 0 < x < L, \tag{5}$$

$$\hat{v}_j(0) = 0, \quad \hat{\psi}_j(0) = 0, \quad \hat{v}_j(L) = 0, \quad \hat{\psi}_j(L) = 0, \quad j = 1,2,3,4.$$

Note that the $v_j(x)$ and $\psi_j(x)$ have already been obtained when solving Eqs. (2) and (3). Hence the derivatives of the dynamic stiffnesses are readily calculated from

$$\left.\begin{aligned} \hat{k}_{1j} &= -\kappa GA\left(\frac{d\hat{v}_j}{dx} - \hat{\psi}_j\right)\Big|_0, \quad \hat{k}_{2j} = -EI\frac{d\hat{\psi}_j}{dx}\Big|_0 \\ \hat{k}_{3j} &= \kappa GA\left(\frac{d\hat{v}_j}{dx} - \hat{\psi}_j\right)\Big|_L, \quad \hat{k}_{4j} = EI\frac{d\hat{\psi}_j}{dx}\Big|_L \end{aligned}\right\}, \quad j = 1,2,3,4. \tag{6}$$

3. Exact static flexural stiffness matrix and its derivative for axially loaded non-uniform Bernoulli–Euler members

The stiffnesses k_{ij} $(i,j = 1,2,3,4)$ for flexure of an axially compressed non-uniform Bernoulli–Euler member are calculated by solving the fourth-order linear ODE BVP of Eq. (7) subject to the four sets of BCs of Eq. (8), where

$$\frac{d^2}{dx^2}\left(EI(x)\frac{d^2v(x)}{dx^2}\right) + P_0\lambda^*\frac{d^2v(x)}{dx^2} = 0, \quad 0 < x < L, \tag{7}$$

$$j = 1: \quad v_j(0) = 1, \quad v_j'(0) = 0, \quad v_j(L) = 0, \quad v_j'(L) = 0, \tag{8a}$$

$$j = 2: \quad v_j(0) = 0, \quad v_j'(0) = 1, \quad v_j(L) = 0, \quad v_j'(L) = 0, \tag{8b}$$

$$j = 3: \quad v_j(0) = 0, \quad v_j'(0) = 0, \quad v_j(L) = 1, \quad v_j'(L) = 0, \tag{8c}$$

$$j = 4: \quad v_j(0) = 0, \quad v_j'(0) = 0, \quad v_j(L) = 0, \quad v_j'(L) = 1. \tag{8d}$$

Here $v_j(x)$ is the lateral displacement, $EI(x)$ is the flexural rigidity, P_0 is a datum value of axial compression, and prime denotes differentiation with respect to x. After the solutions for $v_j(x)$ have been obtained for

$j = 1, 2, 3$ and 4, the buckling stiffnesses can readily be calculated from

$$k_{1j} = (\mathrm{EI}v_j'')'\Big|_0, \quad k_{2j} = -\mathrm{EI}v_j''\Big|_0, \quad k_{3j} = -(\mathrm{EI}v_j'')'\Big|_L, \quad k_{4j} = \mathrm{EI}v_j''\Big|_L, \quad j = 1, 2, 3, 4. \tag{9}$$

The $\hat{k}_{ij}(i, j = 1, 2, 3, 4)$ are obtained by letting $\hat{v} = \partial v/\partial\lambda$ and then differentiating Eqs. (7) and (8) with respect to λ to obtain

$$\frac{\mathrm{d}^2}{\mathrm{d}x^2}\left(\mathrm{EI}(x)\frac{\mathrm{d}^2\hat{v}_j(x)}{\mathrm{d}x^2}\right) + P_0\lambda^*\frac{\mathrm{d}^2\hat{v}_j(x)}{\mathrm{d}x^2} = -P_0\frac{\mathrm{d}^2 v_j(x)}{\mathrm{d}x^2},$$

$$\hat{v}_j(0) = 0, \quad \hat{v}_j'(0) = 0, \quad \hat{v}_j(L) = 0, \quad \hat{v}_j'(L) = 0. \tag{10}$$

Note that the $v_j(x)$ have already been obtained when solving Eqs. (7) and (8). Hence the derivatives of the load-dependent static stiffnesses are readily calculated from

$$\hat{k}_{1j} = (\mathrm{EI}\hat{v}_j'')'\Big|_0, \quad \hat{k}_{2j} = -\mathrm{EI}\hat{v}_j''\Big|_0, \quad \hat{k}_{3j} = -(\mathrm{EI}\hat{v}_j'')'\Big|_L, \quad \hat{k}_{4j} = \mathrm{EI}\hat{v}_j''\Big|_L, \quad j = 1, 2, 3, 4. \tag{11}$$

4. Choice of element lengths

For buckling of uniform clamped ended Bernoulli–Euler struts it is very well known that $P = 4\pi^2\mathrm{EI}/l^2$, where l is the length of the element. By assuming a datum axial force of unity it is permissible to replace P by λ_F and hence the previously established requirement $\lambda_F \geqslant \lambda_u$ gives the upper bound on the permissible element length as

$$l = 2\pi\sqrt{\mathrm{EI}/\lambda_u}. \tag{12}$$

Because increasing $\mathrm{EI}(x)$ must increase λ_F or leave it unaltered, it follows that for the non-uniform element the value of l given by substituting the lowest value of $\mathrm{EI}(x)$ anywhere within l into Eq. (12) forms a lower bound on the maximum value of l that satisfies $\lambda_F \geqslant \lambda_u$. Note that the procedure for determining l is iterative, because l must be known in order to find the lowest $\mathrm{EI}(x)$ within l. Hence using this method for each element except the last one in turn, starting from the left-hand one, gives the positions of all mesh points, although it may be necessary to increase the final element length if it is too short (i.e. it could cause ill-conditioning) by moving the mesh point at its left-hand end an appropriate amount to its left.

A formula for the lowest natural frequency ω_F of a clamped-ended vibrating Timoshenko beam is given in the literature [10]. Additionally, it is a well-established fact that, for any structure, reducing stiffness or adding mass reduces natural frequencies, and hence λ_F. Thus a procedure similar to that given above can be used, by using the formula for ω_F with $\mathrm{EI} = \mathrm{EI}_{\min}$, $\mathrm{GA} = \mathrm{GA}_{\min}$, $m = m_{\max}$ and $I_m = (I_m)_{\max}$, where subscript min (max) denotes the minimum (maximum) value within the length l.

The above forms an important contribution of this paper because it gives the key points of how element lengths, and hence the positions of the mesh points, are found. These key points leave some flexibility over exactly where the mesh points are, because no rule is stated over how the mesh point positions are altered when the rightmost element would otherwise be unacceptably short. Several rules are possible, but the computer program used to obtain the results given in Section 6 below simply did nothing because it worked without difficulty.

Before proceeding it is worth noting that although the number of ODEs is increased as the number of elements increases, these ODEs become easier to solve by the numerical procedure of this paper, because as the elements become shorter their displacements vary less severely. Hence the total computing time may not necessarily increase greatly.

5. Additional theory and information

The axial stiffnesses of the non-uniform beam, both for the vibrating Timoshenko beam and for the axially loaded Bernoulli–Euler beam, are easily obtainable by procedures similar to those used above to find their flexural stiffnesses. It is then possible to set up the $\mathbf{K}(\lambda)$ of Eq. (1) for any chosen plane frame and hence to find

the kth natural frequency λ_k and the associated mode **D** of Eq. (1) by using the recursive inverse iteration procedure of Refs. [3,4]. The member-end displacements are now known via **D**. Therefore, the mode shape on the member can be obtained by solving the same ODEs as in Eqs. (2) or (7), with λ^* being the obtained eigenvalue and the BCs being set to conform to the member-end displacements.

The theory and discussion given above enables the complete method to be presented for computation of a specified number N_f of the leading natural frequencies and associated vibration modes of non-uniform members. The two main contributions of this paper are that the above text has: (i) formulated the ODEs for dynamic stiffnesses of non-uniform members and their derivatives (or their buckling counterparts) and solved them; and (ii) established mesh generation rules for the two problems. Although these are substantial contributions, the algorithm needed to implement them in computer codes has many similarities to that for uniform members in Ref. [3] and so instead of giving the complete algorithm again here only the following differences are mentioned:

(1) The member stiffness and its derivative matrices are computed by solving the governing ODE BVP of each of its elements by using an ODE solver instead of by using closed form formulae.
(2) Different mesh point locations are automatically and adaptively generated for different order frequencies, with the exception of any interior nodes needed to avoid the complete non-uniform member from having a clamped ended eigenvalue very close to λ_u.
(3) J_m is assured to vanish for all elements.

For the complete algorithm, readers are referred to Ref. [3]. Once again the algorithm has been found to work very well and its performance is illustrated by the numerical examples given in the next section.

6. Numerical examples

This section presents five numerical examples showing the excellent performance of the proposed algorithm, which has been implemented in a Fortran 90 program for calculating the flexural vibration of non-uniform Timoshenko beams and the buckling of non-uniform Bernoulli–Euler beams. For greater generality, the examples are presented in dimensionless form. Computation used about 14 decimal digits for floating point number calculations and the error tolerance on the eigenvalues and mode vectors was set to 10^{-8} throughout.

6.1. The three flexural vibration examples and features shared by their solutions

Figs. 1(a)–(c) fully define Examples 1–3 for flexural vibration of Timoshenko beams. Thus the variations with x of $A(x)$ and $I(x)$ for Example 2 are

$$A(x)/L^2 = 0.06\{1-(x/2L)\}, \quad I(x)/L^4 = 8\times 10^{-4}\{1-(x/2L)\}^3, \tag{13}$$

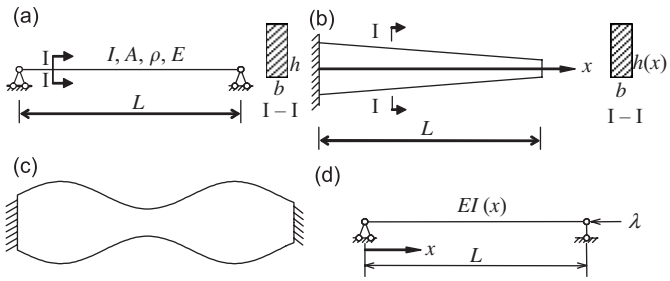

Fig. 1. (a) Example 1: simply supported/simply supported uniform Timoshenko beam with rectangular cross-section, $b/L = 0.1$, $h/L = \eta$, $\eta = 10^{-1}$ or 10^{-6}. (b) Example 2: cantilevered and linearly tapered Timoshenko beam with rectangular cross-section, $b/L = 0.15$, $h(x)/L = 0.4\{1-(x/2L)\}$. (c) Example 3: clamped/clamped Timoshenko beam with rectangular cross-section and sinusoidally varying height, $b/L = 0.15$, $h(x)/L = 0.2\{1+0.5\sin(10x/L)\}$. (d) Example 4: simply supported/simply supported Bernoulli–Euler column, $\mathrm{EI}(x) = \mathrm{EI}_0(1+x/L)^4$. For Examples 1–3, $\kappa = 5/6$ and $G/E = 0.4$.

whereas for Example 3 they are

$$A(x)/L^2 = 0.03\{1 + 0.5\sin(10x/L)\}, \quad I(x)/L^4 = 10^{-4}\{1 + 0.5\sin(10x/L)\}^3. \tag{14}$$

The first ten natural frequencies and modes were computed for the two cases $\eta = 10^{-1}$ and 10^{-6} of Example 1, whereas the first fifty of each were computed for Examples 2 and 3. The $\eta = 10^{-6}$ case was included to illustrate that the present method is not affected by the so-called shear-locking problem at all. The beam was divided into n_g intervals of equal length L/n_g for rigidity and mass value searching, with $n_g = 200$ for Example 1 and $n_g = 500$ for Examples 2 and 3. The initial trial value was 'randomly' set to $\omega^* = 10\sqrt{Eh^2/12\rho L^4}$for Example 1 and to $\omega^* = 10\sqrt{E/\rho L^2}$ for Examples 2 and 3. (Because these trial values are not strictly random, Example 1 was re-run with ω^* set to one tenth of the value above and the errors recorded in Table 1 below were altered negligibly.)

6.2. Presentation and discussion of results for the vibration examples

Analytical results for the kth natural frequency and mode function of Example 1 are given [10] by solving the first line of Eq. (15) to find b_k and then substituting it into the remaining three rows

$$\begin{aligned}
&\frac{b_k}{\sqrt{2}}\sqrt{\frac{\eta^2}{3} + \sqrt{\frac{\eta^4}{36} + \frac{4}{b_k^2}}} = k\pi,\\
&\omega_k = b_k\sqrt{\frac{Eh^2}{12\rho L^4}},\\
&\psi_k(x) = \cos(k\pi x/L),\\
&v_k(x) = k\pi\left(\frac{k^2\pi^2}{b_k^2} - \frac{\eta^2}{12}\right)L\,\sin(k\pi x/L).
\end{aligned} \tag{15}$$

Exact results from Eq. (15) were calculated by using the symbolic software Maple with fifty decimal digits. The first ten of these natural frequencies are given in Table 1 and the errors of the results given by the present method relative to these and to the corresponding exact modes are also included in Table 2. The relative error between the calculated natural frequency ω and the exact value ω_k was calculated as

$$\varepsilon_\omega = \left|\frac{\omega - \omega_k}{\omega_k}\right|. \tag{16}$$

Table 1
Computed results for the flexural vibration of Example 1

k	$\omega_k\left(\div\sqrt{\frac{Eh^2}{12\rho L^4}}\right)$		Relative error in ω_k (i.e. ε_ω)		Absolute mode error	
	$\eta = 10^{-1}$	$\eta = 10^{-6}$	$\eta = 10^{-1}$	$\eta = 10^{-6}$	$\eta = 10^{-1}$	$\eta = 10^{-6}$
1	9.712078861	9.869604401	1.1×10^{-15}	9.0×10^{-16}	3.0×10^{-10}	2.9×10^{-10}
2	37.15925549	39.47841760	2.7×10^{-15}	1.3×10^{-14}	1.7×10^{-9}	2.4×10^{-9}
3	78.41185419	88.82643961	9.5×10^{-13}	1.1×10^{-15}	2.2×10^{-9}	2.6×10^{-9}
4	129.3007567	157.9136704	0	1.6×10^{-13}	4.5×10^{-9}	2.5×10^{-9}
5	186.5185455	246.7401100	0	2.0×10^{-14}	8.3×10^{-10}	1.6×10^{-9}
6	247.7661888	355.3057584	1.2×10^{-14}	8.3×10^{-15}	4.6×10^{-9}	4.5×10^{-9}
7	311.5310273	483.6106156	8.0×10^{-14}	8.3×10^{-12}	5.9×10^{-9}	2.0×10^{-9}
8	376.8356055	631.6546816	2.1×10^{-14}	7.3×10^{-13}	7.8×10^{-10}	3.7×10^{-9}
9	443.0498935	799.4379564	3.2×10^{-14}	1.0×10^{-14}	5.2×10^{-10}	8.0×10^{-9}
10	509.7669406	986.9604399	7.8×10^{-15}	1.6×10^{-12}	4.6×10^{-10}	2.2×10^{-9}

Table 2
Adaptively generated meshes for Examples 2–4

k	Example	n_e	Mesh points (x_i^*/L, $i=0,\ldots,n_e$)
1	2	2	(0 0.798 1)
	3	3	(0 0.466 0.932 1)
	4	2	(0 0.625 1)
2	2	2	(0 0.542 1)
	3	3	(0 0.378 0.692 1)
	4	2	(0 0.415 1)
3	2	3	(0 0.404 0.786 1)
	3	5	(0 0.272 0.466 0.662 0.938 1)
	4	3	(0 0.310 0.845 1)
6	2	5	(0 0.224 0.444 0.662 0.874 1)
	3	7	(0 0.152 0.308 0.436 0.578 0.714 0.886 1)
	4	4	(0 0.155 0.360 0.650 1)
10	2	8	(0 0.138 0.276 0.414 0.550 0.686 0.820 0.954 1)
	3	10	(0 0.108 0.232 0.336 0.434 0.544 0.642 0.752 0.874 0.976 1)
	4	6	(0 0.095 0.210 0.350 0.525 0.745 1)

If there is no exact value available, ω_k is replaced by another reference value in the above equation. The absolute mode errors were calculated as the maximum difference in $\psi(x)$ and $w(x)/L$ on the discrete mesh points x_i ($i=0,1,\ldots,n_g$) with the maximum exact value at any mesh point being set to unity and the corresponding computed value at the same point also being set to unity. It can be seen that it is intrinsic in the present method that it does not suffer from the shear-locking problem and results show that the accuracy requirements are well satisfied.

Table 2 lists selected adaptively generated meshes for Examples 2–4. It shows the number of elements into which the member was divided (n_e) and gives the positions of the mesh points at the element boundaries ($x_0^*, x_1^*, \ldots, x_{n_e}^*$). To obtain a comparator for the natural frequencies given by the present method for Examples 2 and 3, they were also solved by the exact dynamic stiffness method, using 5000 and 10,000 Timoshenko beam elements of constant cross-section for which the constant rigidity and mass values were taken as the original values at the centre of each element, see Table 3. It can be seen that for both of Examples 2 and 3 the results from the present method agree very well with the results given by 10,000 uniform elements. It can also be seen that for Example 2 there is agreement to all 10 significant figures presented with the values obtained by parabolic extrapolation from the results for 5000 and 10,000 elements (using the reciprocal of the number of elements as the abscissa, so that zero corresponds to an infinite number of elements), because the differences between the 5000 and 10,000 element columns in Table 3 is almost exactly three times the differences between the 10,000 element column and the final column, i.e. the present method. Similarly the results for Example 3 from the present method agree very well (almost up to the error tolerance of 10^{-8}) with the results from 10,000 uniform elements and almost always agree to essentially all the significant figures presented with the results extrapolated parabolically from the 5000 and 10,000 results.

6.3. Example 4. Buckling of a simply supported column

The exact critical buckling load and mode shape for the simply supported column defined by Fig. 1(d) are

$$\begin{cases} \lambda_k = 4k^2\pi^2\dfrac{\mathrm{EI}_0}{L^2} \\ v_k(x) = (1+x/L)\sin\dfrac{2k\pi}{(1+x/L)} \end{cases} \quad (k=1,2,\ldots). \tag{17}$$

Table 3
Natural frequencies $\omega_k\left(\div\sqrt{E/\rho L^2}\right)$ of Examples 2 and 3

k	Example 2			Example 3		
	No. of elements		Present	No. of elements		Present
	5000*	10,000*		5000*	10,000*	
1	…3224	…3229	0.403323230	…0754	…0575	1.028940537
2	…3212	…3227	1.500443232	…9687	…9558	2.232669514
3	…4412	…4440	3.088794450	…7201	…7134	3.835177111
4	…8888	…8929	4.823808943	…7479	…7477	5.186177477
5	…8277	…8334	6.650868354	…5337	…5523	7.097895586
10	…5201	…5211	11.486**05214**	…1125	…1134	13.1494**1137**
15	…3174	…3188	17.0573**3193**	…9735	…9740	18.8492**9741**
20	…1942	…1964	22.3895**1971**	…4905	…4928	24.3602**4935**
30	…6873	…6923	34.0684**6940**	…2559	…2554	35.4855**2553**
40	…6927	…6957	45.8825**6968**	…6155	…6137	46.5418**6130**
50	…4239	…4265	56.9152**4274**	…1626	…2067	58.2270**2213**

*Only the last 4 digits are given for these columns to aid comparison with those in the 'present' column to their right (shown bold); the remaining digits are identical.

Table 4
Buckling loads and mode errors of simply supported column

k	$\lambda_k(\div \mathrm{EI}_0/L^2)$	Relative error in λ_k	Absolute error of modes
1	39.47841761	1.6×10^{-10}	1.9×10^{-10}
2	157.9136704	1.9×10^{-10}	5.6×10^{-10}
4	631.6546816	7.0×10^{-11}	1.4×10^{-10}
6	1421.223034	5.3×10^{-11}	4.1×10^{-10}
8	2526.618727	4.8×10^{-11}	2.5×10^{-10}
10	3947.841760	1.9×10^{-11}	4.2×10^{-10}

The first ten buckling loads and modes were computed using the method in this paper with the initial trial value randomly set to $\lambda^* = 100(\mathrm{EI}_0/L^2)$ and with the member divided into $n_g = 200$ intervals of equal length for rigidity value searching. Selected adaptively generated meshes obtained are shown in Table 2 and selected ones of the first ten buckling loads are given in Table 4 along with the error of the present method compared with the exact results of Eq. (18), with the absolute mode error calculated in the same way as for Example 1. Clearly, the accuracy requirements were well satisfied.

6.4. Example 5. Buckling of an optimized clamped–clamped column

For a clamped–clamped column, the problem of determination of the optimal shape was first considered analytically by Tadjbakhsh and Keller [11], using a single mode formulation with no cross-section constraints. However, Olhoff and Rasmussen [12] discovered that the single mode result is not generally optimal, and obtained a better solution based on a bimodal formulation. Their results were confirmed by the first author of the present paper by using an ODE solver approach [13].

According to the definition of this problem, the cross-sections of this column are geometrically similar and similarly oriented so that the moment of inertia I is related to the cross-sectional area A by $I = \gamma A^2$ where the constant γ is a property of the cross-section shape. The column has volume V, length L and Young's modulus E, and is subjected to an axial compressive force, the value of which is P_k at the kth buckling load.

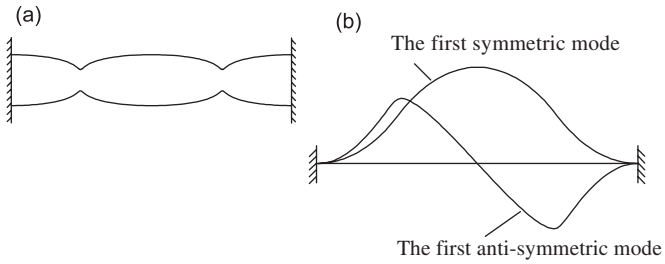

Fig. 2. Example 4. (a) Optimized clamped–clamped column showing the variation of a typical cross-section dimension to plotting accuracy, so that $A(x)$ varies as the square of this dimension. (b) Bimodal shapes obtained by the present method.

Table 5
Buckling loads of clamped–clamped column

	λ_k		
k	Present method	Ref. [12]	ODE solver method [13]
1	52.35625427	52.3563	52.35625427
2	52.35625428	52.3563	52.35625427
3	95.70285107		
4	175.5617089		
5	275.2008589		
6	332.8346468		
7	426.0565157		
8	547.2894105		
9	694.7629409		
10	814.9342154		

The dimensionless cross-sectional area $\alpha(x)$ and buckling loads λ_k are defined by

$$\alpha(x) = A(x)L/V, \quad \lambda_k = P_k L^4/(E\gamma V^2), \tag{18}$$

where the coordinate x ($0 \leqslant x \leqslant 1$) is non-dimensionalized by division by L.

This problem was revisited by using the method proposed in this paper. The optimized shape was calculated in advance by using the ODE-solver method [13] with an error tolerance [9] of 0.5×10^{-10} and is indicated, without detail, in Fig. 2(a). The initial trial value of λ was 'randomly' set to $\lambda^* = 100$. During the computation by the present method, it was found that the first two eigenvalues are very close and the algorithm automatically shifted to the subspace iteration method instead of inverse iteration in solving Eq. (3) and produced the first two solutions simultaneously with no difficulty. The computed results are listed in Table 5. It is evident that the solutions agree very well with the comparator results shown for the first two eigenvalues, with the very slight difference from the results of Ref. [12] being due to the adopted shape being presented to the present method in a numerical form rather than a closed analytic one. Finally, the first two modal shapes computed by the present method are shown in Fig. 2(b).

7. Concluding remarks

In this paper, the exact dynamic stiffness method (DSM) has been further extended to vibration of non-uniform Timoshenko beams and buckling of non-uniform Euler members. For the method presented, the following final remarks are made.

7.1. Exactness

The word 'exact' can never be strictly applied to computer methods both because the computer works to a finite accuracy and also because even precise analytical solutions often involve functions such as sine and cosine which are evaluated from series. Therefore, 'exact' is used here to describe methods which achieve machine accuracy less a very limited allowance for a normal amount of ill-conditioning. In this sense, because the method presented is a numerical implementation of the exact DSM, it is an exact method because it uses a standard adaptive ODE solver to compute dynamic stiffnesses and their derivatives to either a user-specified accuracy or the maximum accuracy allowed by the computer. This contrasts with many other methods, e.g. the extensively used FEM would very rarely (if ever) use, or possibly be able to use, sufficient elements for the discretization errors (plus any ill-conditioning errors due to using very small elements) for its accuracy to ever approach machine accuracy. Note too that the method presented, unlike FEM, allows the accuracy required to be preset in data.

7.2. Efficiency

The efficiency of the proposed method depends on several factors. An important one is the efficiency of the adopted ODE solver. So far as is known the solver used is one of the best to use but if a more efficient ODE solver could be found it would raise the overall efficiency of the method. If very high accuracy is required the method presented is manifestly more efficient than using an astronomically large number of finite elements, which incidentally would probably need to be monitored carefully lest they cause ill-conditioning. As an indication of the speed of the present method, the code used (which has not been optimized) took 2.413, 1.973, 21.250 and 20.850 s to solve Examples 1 (for $\eta = 10^{-1}$ and 10^{-6}), 2 and 3, respectively, when using an IBM Notebook PC with a Pentium M 1.7 GHz CPU.

7.3. Reliability

High reliability is achieved via a sophisticatedly designed algorithm. The use of a state-of-the-art ODE solver guarantees the quality of the computed stiffnesses and their derivatives, even for challenging problems, and the use of the W–W algorithm to bound the sought eigenvalues guarantees that no eigenvalues are missed.

7.4. Generality

The calculation of the dynamic stiffnesses and their derivatives by using an ODE solver is a general method which can be easily extended to cover more general problems, including the three-dimensional frameworks briefly discussed at the end of Section 1. Similarly, the mesh generation can be generalized to other problems, e.g. non-uniform beams on non-uniform elastic foundations, as long as valid element length rules can be established.

Acknowledgements

The authors gratefully acknowledge financial support from the National Natural Science Foundation of China, the Ministry of Education of China (No. 704003), the Engineering and Physical Sciences Research Council (grant number GR/R05406/01) and the Royal Academy of Engineering.

References

[1] W.H. Wittrick, F.W. Williams, A general algorithm for computing natural frequencies of elastic structures, *Quarterly Journal of Mechanics and Applied Mathematics* 24 (1971) 263–284.

[2] F.W. Williams, W.H. Wittrick, An automatic computational procedure for calculating natural frequencies of skeletal structures, *International Journal of Mechanical Sciences* 12 (1970) 781–791.

[3] S. Yuan, K. Ye, F.W. Williams, D. Kennedy, Recursive second order convergence method for natural frequencies and modes when using dynamic stiffness matrices, *International Journal for Numerical Methods in Engineering* 56 (2003) 1795–1814.

[4] M.S. Djoudi, D. Kennedy, F.W. Williams, S. Yuan, K. Ye, Exact substructuring in recursive Newton's method for solving transcendental eigenproblems, *Journal of Sound and Vibration* 280 (2005) 883–902.
[5] S. Pruess, C.T. Fulton, Mathematical software for Sturm-Liouville problems, *ACM Transactions on Mathematical Software* 19 (1993) 360–376.
[6] P.B. Bailey, W.N. Everitt, A. Zettl, Algorithm 810: the SLEIGN2 Sturm-Liouville code, *ACM Transactions on Mathematical Software* 27 (2001) 143–192.
[7] NAG Fortran Library, Vol. 2, Numerical Algorithms Group Ltd., Oxford, 1988.
[8] L. Greenberg, M. Marletta, The code SLEUTH for solving fourth order Sturm-Liouville problems, *ACM Transactions on Mathematical Software* 23 (1997) 453–497.
[9] U. Ascher, J. Christiansen, R.D. Russell, Algorithm 569, COLSYS: collocation software for boundary value ODEs[D2], *ACM Transactions on Mathematical Software* 7 (1981) 223–229.
[10] W.P. Howson, F.W. Williams, Natural frequencies of frames with axially loaded Timoshenko members, *Journal of Sound and Vibration* 26 (1973) 503–515.
[11] I. Tadjbakhsh, J.B. Keller, Strongest columns and isoperimetric inequalities for eigenvalues, *Journal of Applied Mechanics* 29 (1962) 159–164.
[12] N. Olhoff, S.H. Rasmussen, On single and bimodal optimum bucking loads of clamped columns, *International Journal of Solids and Structures* 13 (1977) 605–614.
[13] S. Yuan, Application of ODE techniques and software to determination of optimum buckling loads of clamped columns, *Computers and Structures* 39 (1991) 391–398.